JACS
JOURNAL OF THE AMERICAN CHEMICAL SOCIETY

COMMUNICATION

pubs.acs.org/JACS

Anisochronous Dynamics in a Crystalline Array of Steroidal Molecular Rotors: Evidence of Correlated Motion within 1D Helical Domains

Braulio Rodríguez-Molina,[†,§] Norberto Farfán,[‡] Margarita Romero,[‡] J. Manuel Méndez-Stivalet,[‡] Rosa Santillan,[*,†] and Miguel A. Garcia-Garibay[*,§]

[†]Departamento de Química, Centro de Investigación y de Estudios Avanzados del IPN, México D.F. Apdo. Postal 14-740, 07000 México
[‡]Facultad de Química, Departamento de Química Orgánica, Universidad Nacional Autónoma de México, México D.F. 04510, México
[§]Chemistry and Biochemistry Department, University of California, Los Angeles, California 90095, United States

Supporting Information

ABSTRACT: We describe the solid-state dynamics of a molecular rotator (**2**) consisting of a *p*-phenylene rotor flanked by two ethynyl steroidal moieties that act as a stator. Single-crystal X-ray diffraction analysis of polymorph I revealed a packing motif containing 1D columns of nested rotors arranged in helical arrays (space group $P3_2$) with the central phenylenes disordered over two sites related by an 85° rotation about their 1,4-axes. Unexpected line shapes in quadrupolar-echo ^{2}H NMR measurements between 155 and 296 K for the same polymorph with a deuterated phenylene isotopologue (**2**-d_4) were simulated by trajectories involving fast (>10^8 s^{-1}) 180° rotation (twofold flips) in each of the two rotationally disordered sites and slower exchange (2×10^4 to 1.5×10^6 s^{-1}) between them. A negative activation entropy and a low enthalpic barrier for the slower 85° exchange are interpreted in terms of highly correlated processes within the 1D helical domains.

Crystalline arrays of molecular rotors are attractive for applications in materials science and nanotechnology and are a promising entry into the field of artificial molecular machines.[1,2] Over the past few years, in search of structures with low rotational barriers in the solid state, we have investigated molecular rotors that emulate the structure of macroscopic gyroscopes. Several structures have been designed in which phenylene groups act as rotators (shown in red in Figure 1) and bulky substituents act as stators (shown in blue). The concept is illustrated in Figure 1 with 1,4-bis[3,3,3-(4-*tert*-butylphenyl)-ethynyl]benzene (**1**).[3,4] Using variable-temperature (VT) solid-state ^{2}H NMR spectroscopy with rotator-labeled samples, we have determined their exchange rates and rotational trajectories, which consist of angular displacements of 180°, also known as "twofold flips". While we have shown that molecular rotors with bulky stators lead to room-temperature exchange rates in the gigahertz (10^{12} s^{-1}) regime,[5] it is also desirable to identify crystalline rotor arrays with more complex dynamics, such as correlated motions and multiple rotational potentials.

Here we report the internal dynamics of a new molecular rotor (**2**) built with the steroid mestranol. We recently began to explore the use of steroids as molecular stators,[6] motivated by their rigid structures and chiral nature.[7] While examples reported in a recent article suggested a promising platform for obtaining noncentrosymmetric crystals, the new mestranol rotor displayed a remarkable and unexpected dynamic behavior. A detailed analysis of VT ^{2}H NMR data acquired between 155 and 296 K revealed spectra that are very different from those expected for rotation in a simple symmetric potential.

Figure 1. Molecular rotors intended to emulate the structure and function of macroscopic gyroscopes. The stators and axles of rotation are shown in blue and the phenylene rotators are shown in red.

On the basis of its single-crystal X-ray structure and activation parameters (described in detail below), we propose an anisochronous dynamic model involving collective rotator reorientation in molecules that stack in helical columns and a fast ($\geq 10^8$ s^{-1}) 180° rotation at each of the two slowly exchanging sites. The suggested collective transformation is reminiscent of a phase transition within the columnar 1D domains.

The synthesis of compound **2** was accomplished by a Pd(0) Sonogashira cross-coupling reaction of mestranol with 1,4-diiodobenzene [see the Supporting Information SI]. The deuterated analogue **2**-d_4 was obtained with 1,4-dibromobenzene-d_4. The ^{1}H NMR spectrum of compound **2** in solution showed an aromatic peak at 7.39 ppm that was correlated with a signal at 131.7 ppm in the ^{13}C NMR spectrum, which was assigned to the central rotator. The ^{13}C NMR spectrum of compound **2** in solution displayed a number of peaks accounting for only half of the molecule, suggesting a time-averaged C_2-symmetric structure.[8]

The very first crystallization of rotor **2** from CH_2Cl_2/*N*,*N*-dimethylformamide (DMF) concomitantly yielded two crystal forms (I and II) that were fully characterized by single-crystal X-ray diffraction (XRD) (Figure 2). All subsequent crystallizations with pure solvents, binary mixtures, and a wide range of

Received: January 21, 2011
Published: April 27, 2011

dx.doi.org/10.1021/ja2006274 | *J. Am. Chem. Soc.* 2011, 133, 7280–7283

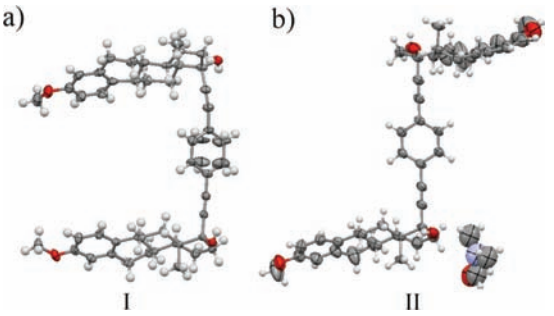

Figure 2. Molecular structures of the crystalline forms of mestranol rotor **2**: (a) solvent-free form I; (b) DMF-solvated form II.

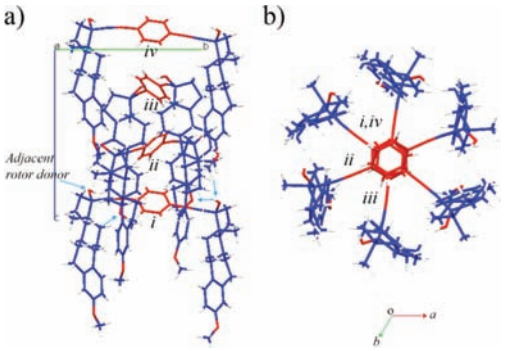

Figure 3. (a) Columnar 1D arrangement of nested molecular rotors in crystals of **2** (form I); only one of the sites for the central phenylene is shown. (b) View down the *c* crystallographic 3_2 axis.

modifications yielded only form I. Diffraction data for the solvent-free form I were solved in the space group $P3_2$,[9] and those for form II were solved in the space group $P2_12_12_1$.[10] Structural details for the disappearing[11] polymorph II are included in the SI. The molecular structure of form I can be described by a model that includes disorder of the central phenylene over two positions related by an 85° rotation about the alkyne axle. The two sites (A and B) are not equivalent, and their population at 173 K is 47:53. The structure of the steroidal portions is consistent with those of pure mestranol,[12] with a half-chair conformation of ring B and ideal chair and envelope arrangements for rings C and D, respectively. As illustrated in Figure 2a, the axial alkyne linkage at C17 has a small deviation from orthogonality with respect to the plane of the steroids, and the "U" shape of the latter creates a cavity that shields one face of the phenylene rotator.

The packing arrangement of form I (Figure 3) consists of helical columns of nested rotors. Each column represents a 1D helical stack that propagates along the 3_2 screw axis, which passes through the center of the phenylene rotators and places the dialkyne axles roughly parallel to the *ab* plane (Figure 3b). Molecules within the column interact by hydrogen bonding[13] in such a manner that the −OH group at C17 acts as hydrogen-bond donor to the oxygen of a methoxy group in a neighboring molecule in the stack (Figure 3a). This architecture results in a relatively long distance between adjacent phenylene rotators along the column, with a center-to-center distance of 4.91 Å.

Before characterization by solid-state NMR analysis, the phase purity of form I was established by thermogravimetric analysis (TGA) and powder XRD (see the SI). The ^{13}C cross-polarization magic-angle-spinning (CPMAS) NMR spectrum at 295 K showed

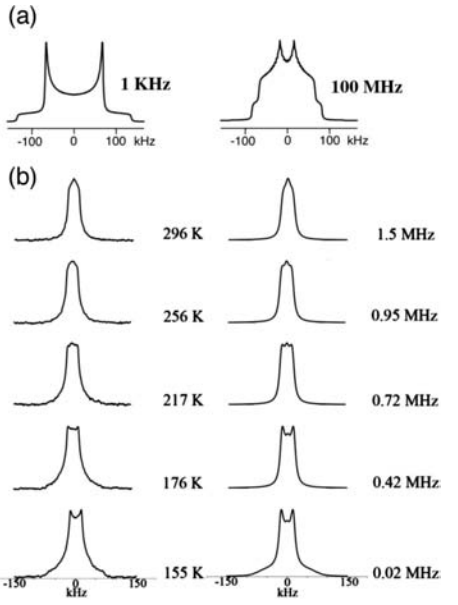

Figure 4. (a) Simulated VT quadrupolar-echo ^{2}H NMR spectra for a dynamic process involving 180° jumps of a *p*-phenylene in the slow (1 kHz) and fast (100 MHz) exchange regimes. (b) (left) Representative experimental spectra obtained with compound **2**-d_4 (form I) from 155 to 296 K. (right) Spectra calculated with a model that considers two concurrent dynamics with different rates, k_{180} at 100 MHz (180° jumps) and k_{85} (85° jumps) at the frequencies listed.

well-resolved pairs of signals for various steroidal carbons, indicating that the two steroids are not equivalent, in accordance to the crystallographic data. The four crystallographically nonequivalent and orientationally disordered C−H carbons of the phenylene rotator appeared as a narrow peak at 131.5 ppm with a half width of ca. 95 Hz, suggesting that fast exchange between positions related by rotation about the dialkyne axis may occur. ^{13}C CPMAS NMR spectra acquired under conditions of interrupted ^{1}H decoupling showed that the signal of the phenylene rotator did not become dephased (see the SI), as expected for a rapid dynamic process that reduces the magnitude of the C−H coupling.[14] Subsequent ^{13}C CPMAS NMR experiments down to 155 K showed only a slight broadening of every carbon signal (see the SI), suggesting that fast phenylene rotation remained even at that temperature.

The rotational exchange of rotor **2** was subsequently explored using quadrupolar-echo ^{2}H NMR spectroscopy using polycrystalline powder samples of **2**-d_4. The dynamic range covered by this method spanned 5 orders of magnitude, with exchange frequencies k_{ex} varying from ca. 10^3 to 10^8 s^{-1} (1 kHz to 100 MHz) and spectral line shapes dependent on the trajectories of motion and their characteristic exchange frequencies. As indicated in Figure 4a, static deuterons display a broad spectrum known as a Pake pattern spanning ca. 260 kHz with two maxima ca. 130 kHz apart. Phenylene rotation in the fast-exchange limit ($k_{ex} \geq 10^8$ s^{-1}) typically occurs in the form of 180° jumps (or twofold flips) and results in a narrower spectrum with a distance of only ca. 30 kHz between the two maxima. Surprisingly, instead of the typical twofold-flipping spectra, samples of rotor **2**-d_4 measured at 295 K produced a very narrow line shape (Figure 4b) with a maximum in the center and a half width of only ca. 32 kHz, suggesting a rotational potential with more than two minima and/or a complex trajectory.

dx.doi.org/10.1021/ja2006274 |*J. Am. Chem. Soc.* 2011, 133, 7280–7283

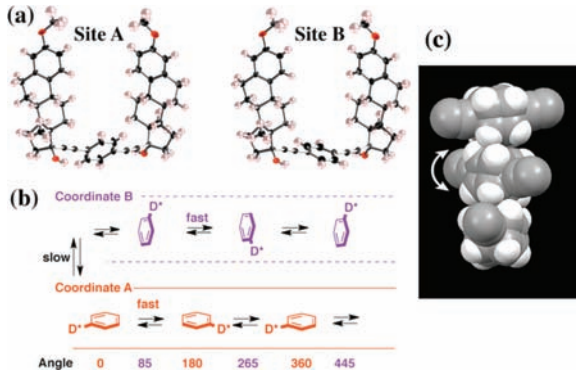

Figure 5. (a) Rotors corresponding to sites A and B are dephased by 85°. (b) Site-exchange model including rotors undergoing rapid ($\geq 10^8$ s^{-1}) twofold flipping (180° rotation) within sites A or B with slow (10^3–10^6 s^{-1}) switching between these sites. (c) Portion of the rotor array illustrating the two sites of the disorder obtained by removing the X-ray coordinates of the steroidal stator. A simple 85° oscillation as suggested by the arrows was not supported by the ^{2}H NMR results.

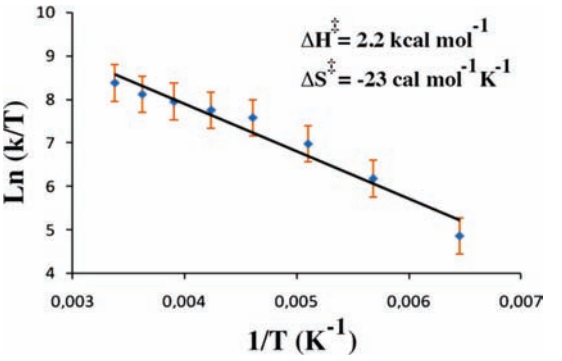

Figure 6. Eyring plot for the phenylene-d_4 site exchange in compound **2** (form I) derived from the VT ^{2}H solid-state NMR experiments (R^2 = 0.9557). The corresponding activation enthalpy was 2.2 kcal/mol.

While intuition suggest a fast exchange process between sites connected by the shorter angular displacements of 85°, the experimental spectra in Figure 4 could not be fit with a model that considered either back-and-forth oscillations of 85° or jumps between all of the disordered sites at a single rate (see the SI).[15] Furthermore, the spectra could not be simulated using any model that considered rotation in a symmetric *n*-fold potential. Considering the two X-ray minima shown in Figure 5a, we decided to explore models assuming anisochronous 85° and 180° exchange trajectories. We first noticed that simulations with any combination of fast 85° jumps and slow 180° rotations failed to match the results from the experiments. However, a model based on fast ($k_{180} \geq 10^8$ s^{-1}) 180° exchange within each site (A ↔ A′ and B ↔ B′) and slower ($k_{85} = 10^3$–10^6 s^{-1}) 85° jumps between the sites related by disorder (A ↔ B and B ↔ A) reproduced the experimental data very well. As indicated in Figure 5b, a given trajectory could start with a fast twofold flipping motion in site A (i.e., 0 ↔ 180 ↔ 360 ↔ etc.) followed by a switch to site B (i.e., 85 ↔ 265 ↔ 85 ↔ etc.) with frequencies varying from 20 kHz at 155 K to 1.5 MHz at 296 K. This model accounted for all of the features of the experimental spectra, including the relatively narrow line width, the single maximum at 296 K that transformed into two close peaks as the sample was cooled to 217 K, and the appearance of a broad feature at the baseline below ca. 176 K. The simulations in Figure 4 were sensitive to variations of greater than ±2° in the slower process, matching the XRD angle between the two sites remarkably well.

An Arrhenius plot based on the temperature and frequency data for the slower switching process gave an activation energy of only 2.6 kcal/mol and a pre-exponential factor of 1.2×10^8 s^{-1}. Since the pre-exponential factor (or attempt frequency) for an elementary phenylene rotation is associated with a libration frequency of ca. 10^{12} s^{-1},[3−5] a pre-exponential factor that is 4 orders of magnitude smaller indicates a complex mechanism. An Eyring plot (Figure 6) gave a low activation enthalpy of 2.2 kcal/mol and an activation entropy of ca. −23 cal mol^{-1} K^{-1}, suggesting that switching between sites A and B must be mediated by a highly organized exchange mechanism (Figure 5b). We interpret the results in Figures 4 and 6 as indicative of a highly correlated process within the 1D channel structure of mestranol rotor **2**. A model that considers the dynamics of the rotor within a potential determined by hypothetically static neighbors suggests oscillations between disordered positions (Figure 5c) and fails to account for the observed results. In fact, the potential of any test rotor is time-dependent and modulated by oscillations and rotations of neighboring rotators along the chain. To visualize the complexities arising from the dynamics within the helical columns, one may consider the range of rotational configurations[16] available to the neighbors of a test rotor. Shown in Figure 7a is an illustration of the potentials that occur as a function of three such configurations. The potential energy shown in blue represents a configuration where both close neighbors adopt an angle of 90° with respect to the channel axis (i.e., 90°/90°), which creates adverse steric interactions only when the central rotor angle is close to 0° or 180°, as illustrated by representations in blue at the bottom of Figure 7a. Shown in red is the potential expected when both neighbors adopt angles of 0° (i.e., 0°/0°), which restricts the central rotators to very narrow displacements around an angle of 90° with respect to the helix channel, as shown in red by the representation in the center of the corresponding potential. The potential shown in black represent the equilibrium configuration of the adjacent rotators as determined by X-ray analysis, which would allow for oscillation between ca. 50° and 135°. Since there are many other configurations, it is clear that the rotational potential is not static. As shown by the heavy line in Figure 7b, we propose that the effective potential is dynamically determined by the correlated motion of two or more rotators along the column, with oscillations ranging from 90°/90° to 0°/0°, relative to the vertical channel axis. A plausible mechanism for the observed 180° rotation that retains the angular configuration of the three rotators in the model is suggested by the representations at the bottom of Figure 7a with the orientation of the central rotator indicated with a purple dot. This qualitative analysis suggests that mestranol rotor **2** should provide an interesting testing ground for molecular dynamics simulations, which may help establish the relation between its time- and space-averaged X-ray structure and rotational dynamics. We also hope that molecular dynamics simulations will give insight into the mechanism required to switch between the two equilibrium sites and the possible formation of rotary domains.

In conclusion, crystals of steroidal rotor **2** constitute an ideal and unprecedented system for studying correlated rotational dynamics in the solid state. VT ^{2}H NMR spectra and line shape simulations revealed that its rotational dynamics consist of two anisochronous processes involving a relatively slow switching between two distinct twofold flipping trajectories in the fast-exchange regime. We believe that the short distance between adjacent rotators will be ideal for analyzing dipole−dipole interactions with *o*-difluorophenylene

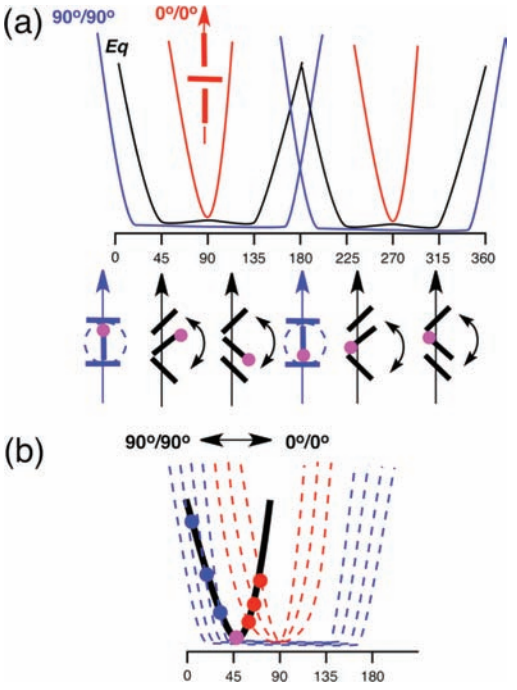

Figure 7. (a) Hypothetical variations in the rotational potential of a central rotor as a function of the *static* rotational angles of its closest neighbors in the channel. Potentials in blue and red represent configurations where the planes of the two neighbors are either orthogonal (blue) or parallel (red) to the vertical channel axis. The potential in black represents the equilibrium configuration determined by XRD (as in Figure 5c). The angles available to the central rotor and a plausible mechanism for a 180° flip are illustrated at the bottom. (b) Illustration of a plausible effective rotational potential (black line) that results from the correlated motion of the rotator's closest neighbors.

rotators with the symmetry of an isostructural lattice guiding the formation of 1D helical stacks. Experiments to test these and other expectations are currently underway.

■ ASSOCIATED CONTENT

Supporting Information. Experimental procedures, spectral and X-ray data, DSC and TGA analyses, VT ^{13}C CPMAS solid-state NMR spectra, powder XRD pattern of form I, and crystallographic data (CIF). This material is available free of charge via the Internet at http://pubs.acs.org.

■ AUTHOR INFORMATION

Corresponding Author
rsantill@cinvestav.mx; mgg@chem.ucla.edu

■ ACKNOWLEDGMENT

B.R.-M. thanks CONACYT for a scholarship. We thank V. González for solution NMR spectra, G. Cuéllar for mass spectrometry data, and M. A. Leyva for X-ray diffraction experiments. Work at UCLA was supported by NSF Grant DMR0605688 and Creativity Extension DMR0937243.

■ REFERENCES

(1) (a) Browne, W. R.; Feringa, B. L. *Nat. Nanotechnol.* **2006**, *1*, 25. (b) Horinek, D.; Michl, J. *Proc. Natl. Acad. Sci. U.S.A.* **2005**, *102*, 14175. (c) de Jonge, J. J.; Ratner, M. A.; de Leeuw, S. W. *J. Phys. Chem. C* **2007**, *111*, 3770. (d) Shirai, Y.; Morin, J.-F.; Sasaki, T.; Guerrero, J. M.; Tour, J. M. *Chem. Soc. Rev.* **2006**, *35*, 1043. (e) Tierney, H. L.; Baber, A. E.; Jewell, A. D.; Iski, E. V.; Boucher, M.; Sykes, E. C. H. *Chem.—Eur. J.* **2009**, *15*, 9678. (f) Rabe, K. M.; Dawber, M.; Lichtensteiger, C.; Ahn, C. H.; Triscone, J.-M. *Top. Appl. Phys.* **2007**, *105*, 1. (g) Garcia-Garibay, M. A. *Angew. Chem., Int. Ed.* **2007**, *46*, 8945.

(2) (a) Horiuchi, S.; Tokunaga, Y.; Giovanetti, G.; Picozzi, S.; Itoh, H.; Shimano, R.; Kumai, R.; Tokura, Y. *Nature* **2010**, *463*, 789. (b) Akutagawa, T.; Koshinaka, H.; Sato, D.; Takeda, S.; Noro, S. I.; Takahashi, H.; Kumai, R.; Tokura, Y.; Nakamura, T. *Nat. Mater.* **2009**, *8*, 342.

(3) (a) Karlen, S. D.; Garcia-Garibay, M. A. *Top. Curr. Chem.* **2006**, *262*, 179. (b) Khuong, T. A.; Nuñez, J. E.; Godinez, C. E.; García-Garibay, M. A. *Acc. Chem. Res.* **2006**, *39*, 413. (c) Garcia-Garibay, M. A. *Proc. Natl. Acad. Sci. U.S.A.* **2005**, *102*, 10771.

(4) (a) Khuong, T.-A. V.; Zepeda, G.; Ruiz, R.; Kahn, S. I.; Garcia-Garibay, M. A. *Cryst. Growth Des.* **2004**, *4*, 15. (b) Godinez, C. E.; Garcia-Garibay, M. A. *Cryst. Growth Des.* **2009**, *9*, 3124.

(5) Karlen, S. D.; Reyes, H.; Taylor, R. E.; Khan, S. I.; Hawthorne, M. F.; Garcia-Garibay, M. A. *Proc. Natl. Acad. Sci. U.S.A.* **2010**, *107*, 14973.

(6) Rodríguez-Molina, B.; Pozos, A.; Cruz, R.; Romero, M.; Flores, B.; Farfán, N.; Santillan, R.; Garcia-Garibay, M. A. *Org. Biomol. Chem.* **2010**, *8*, 2993.

(7) Moulton, B.; Zaworotko, M. J. In *Crystal Engineering: From Molecules and Crystals to Materials*; Braga, D., Grepioni, F., Orpen, A. G., Eds.; Kluwer: Dordrecht, The Netherlands, 1999.

(8) The observed ^{13}C chemical shifts of the steroid backbone agree with the reported values. See: (a) Sedee, A. G. J.; Vanhenegouwen, G.; Devries, M. E.; Erkelens, C. *Steroids* **1985**, *45*, 101. (b) Ciuffreda, P.; Ferraboschi, P.; Verza, E.; Manzocchi, A. *Magn. Reson. Chem.* **2001**, *39*, 648. (c) Blunt, J. W.; Stothers, J. B. *Org. Magn. Reson.* **1977**, *9*, 439. (d) Kirk, D. N.; Toms, H. C.; Douglas, C.; White, K. A.; Smith, K. E.; Latif, S.; Hubbard, R. W. P. *J. Chem. Soc., Perkin Trans. 2* **1990**, *9*, 1567.

(9) Form I from DMF. Data collected at 173 K. $C_{48}H_{54}O_4$; MW = 694.91; space group $P3_2$; a = 14.7945(6) Å, b = 14.7945(6) Å, c = 14.7246(4) Å, α = 90°, β = 90°, γ = 120°; V = 2791.09(18) Å^3; Z = 3; ρ_{calcd} = 1.221 Mg/m^3; $F(000)$ = 1122; λ = Å, μ(Mo Kα) = 0.71073 mm^{-1}; T = 173(2) K; crystal size = 0.30 mm × 0.15 mm × 0.12 mm; 15 100 reflns collected ($3 \le \theta \le 27°$), 7906 independent reflns [R(int) = 0.0508]; max/min residual electron density 0.23/−0.198 e Å^{-3}; R_1 = 0.0512 [$I > 2\sigma(I)$], wR_2 = 0.0925 (all data).

(10) Form II from CH_2Cl_2/DMF. Data collected at 295 K. $C_{48}H_{54}O_4 \cdot$DMF; MW = 768.01; space group $P2_12_12_1$; a = 12.260(3) Å, b = 18.528(4) Å, c = 19.062(4) Å, α = 90°, β = 90°, γ = 90°; V = 4330.1(15) Å^3; Z = 4; ρ_{calcd} = 1.17 Mg/m^3; $F(000)$ = 1547.4; λ = Å, μ(Mo Kα) = 0.71073 mm^{-1}; T = 293(2) K; crystal size = 0.30 mm × 0.25 mm × 0.25 mm; 25 475 reflns collected ($1 \le \theta \le 27°$), 9369 independent reflns [R(int) = 0.0538]; max/min residual electron density 0.31/−0.28 e Å^{-3}; R_1 = 0.074 [$I > 2\sigma(I)$], wR_2 = 0.212 (all data).

(11) Dunitz, J. D.; Bernstein, J. *Acc. Chem. Res.* **1995**, *28*, 193.

(12) (a) Steiner, T.; Lutz, B.; van der Maas, J.; Veldman, N.; Schreurs, A. M. M.; Kroon, J.; Kanters, J. A. *Chem. Commun.* **1997**, 191. (b) Steiner, T.; Veldman, N.; Schreurs, A. M. M.; Kanters, J.; Kroon, J. *J. Mol. Struct.* **1998**, *447*, 43.

(13) (a) Taylor, R.; Kennard, O. *J. Am. Chem. Soc.* **1982**, *104*, 5063. (b) Steiner, T. *Chem. Commun.* **1997**, 727. (c) Desiraju, G. *Acc. Chem. Res.* **1996**, *29*, 441.

(14) Alemany, L. B.; Grant, D. M.; Alger, T. D.; Pugmire, R. J. *J. Am. Chem. Soc.* **1983**, *105*, 6697.

(15) (a) Nishikiori, S. I.; Soma, T.; Iwamoto, T. *J. Inclusion Phenom. Mol. Recognit. Chem.* **1997**, *27*, 233. (b) Macho, V.; Brombacher, L.; Spiess, H. W. *Appl. Magn. Reson.* **2001**, *20*, 405.

(16) While the corresponding structures are different conformations in the organic structural sense, we have used the term configuration in the statistical mechanics sense to highlight their relation to the entropy of the system.